Appl. Phys. A 74, 13–17 (2002) / Digital Object Identifier (DOI) 10.1007/s003390100993

Applied Physics A
Materials
Science & Processing

Size evolution and photoluminescence of silicon nanocrystallites in evaporated SiO_x thin films upon thermal processing

U. Kahler*, H. Hofmeister

Max Planck Institute of Microstructure Physics, Weinberg 2, 06120 Halle, Germany

Received: 3 July 2001/Accepted: 6 August 2001/Published online: 17 October 2001 –

Abstract. Silicon suboxide thin films have been fabricated by physical vapor deposition of silicon monoxide in vacuum at controlled oxygen partial pressure. These films undergo a phase separation into silicon- and oxygen-enriched regions upon thermal processing. At temperatures around 900 °C, the onset of Si nanocrystallite formation is observed, regardless of film stoichiometry. With increasing initial oxygen content of the films, the mean size of created nanocrystallites decreases whereas the corresponding photoluminescence emission blueshifts. The photoluminescence intensity increases with increasing annealing temperature up to 1050 °C. Upon resonant excitation at low temperatures, the photoluminescence exhibits phonon replica signature. Therefore, the emission may be attributed to excitonic recombination in the nanocrystallites.

PACS: 61.16.-d; 61.46.+w; 78.66.-w; 81.15.Ef; 81.40.Ef

Since 1990, when the first investigations of the luminescence and quantum confinement in porous silicon were reported [1, 2], light emission from nanostructured silicon has been extensively investigated. In the following years, many alternative techniques for synthesis of Si nanocrystallites in oxide matrix were explored such as high-dose Si-ion implantation in SiO_2 [3, 4], cosputtering of Si and SiO_2 [5, 6], laser ablation of Si, solely or together with SiO_2 [7, 8], gas-phase evaporation of silicon monoxide (SiO) [9, 10] and plasma-assisted chemical vapor deposition of silicon suboxide (SiO_x) [11, 12]. Another powerful technique for producing Si nanocrystallites in a SiO_2 matrix is, as demonstrated in our previous studies, thermal evaporation of SiO [13, 14]. First results on the photoluminescence (PL) emission were reported elsewhere [15]. In this paper, we present a comprehensive view of the luminescence properties of Si nanocrystallites formed upon high-temperature annealing of SiO_x films ($1 \leq x \leq 2$) produced by reactive evaporation of SiO in high vacuum.

*Corresponding author.
(Fax: +49-345/551-1223, E-mail: kahler@mpi-halle.mpg.de)

1 Experimental

Amorphous thin films of SiO_x were fabricated by evaporation of commercially available SiO (Balzers) from two Ta boats in high vacuum. The material was deposited onto rotating 10-cm Si(100)-wafer substrates heated to 100 °C by rear illumination with tungsten-halide lamps. To achieve uniform film thickness, the angle between the evaporators and the substrate center was fixed at 53°. The base pressure of the system was held at 2×10^{-7} mbar. A certain oxygen partial pressure was achieved by admitting high-purity oxygen gas into the evaporation chamber. Rutherford backscattering (RBS) measurements proved that under otherwise identical conditions, the final film stoichiometry was a monotonic function of the oxygen partial pressure [14, 15]. Accordingly, the film stoichiometry parameter x could be adjusted in the range between 1 and 2 by fixing the evaporation rate to 12 nm/min and changing the oxygen partial pressure appropriately. The oxygen partial pressure was varied in six steps from 2×10^{-7} mbar to 1×10^{-4} mbar leading to SiO_x thin films named O1 to O6. After deposition, the films were annealed in a conventional quartz-tube furnace in order to induce the phase separation into silicon- and oxygen-enriched regions, respectively.

The formation of nanocrystallites was investigated by high-resolution electron microscopy (HREM) using a JEM 4000 EX (Jeol) operating at 400 kV. The cross-section preparation technique was applied to enable not only characterization of size, size distribution and shape of Si nanocrystallites, but also of their spatial distribution within the films. PL spectra under UV excitation (UV line of a He–Cd laser at 325 nm) were measured at room temperature by using a grating spectrometer and two different photomultiplier tubes (Hamamatsu R928 and R5108). To obtain more detailed information on the origin of the PL emission, additional PL measurements at low temperature (4 K) were carried out. The experimental

setup of the measurements together with a theoretical background were presented by Kovalev et al. [16]. The procedure had initially been proposed by Calcott et al. [17].

2 Results and discussion

2.1 Structural characteristics

Besides residual gas pressure and evaporation rate, the geometry of the evaporation setup has a large influence on thin-film structural characteristics. Films evaporated under oblique incidence (average angle of 53° between substrate center and incident molecules) exhibit a certain porosity and, after removal from the vacuum system, they tend to attract water from the ambient. This causes an optical absorption in the infrared with maxima at 3500 cm^{-1} and around 2200 cm^{-1} due to the formation of Si–H and –OH groups, respectively. This phenomenon is caused by a self-shadowing effect due to the oblique evaporation [18]. It is not observed with films produced by deliberately using vertical evaporation geometry [19]. The oblique evaporation, however, has been used to obtain films of uniform thickness over the whole substrate. This way, the thickness inhomogeneity on a 10-cm wafer could be reduced to less than 0.5%. Annealing at temperatures higher than 600 °C caused a densification of the films and a loss of –OH groups by water desorption. Such a densification effect has been reported also for SiO_2 films [20]. After annealing at high temperatures the films are stable and do not adsorb any water from the ambient, i.e. they are dense films just as those deposited at vertical evaporation geometry.

HREM revealed the formation of Si nanocrystallites only upon annealing at 900 °C. At this temperature rather few crystallites were found. A higher density was achieved by raising the annealing temperature to about 1000 °C. To illustrate these results, Fig. 1 shows selections of HREM micrographs with Si nanocrystallites in SiO_2 matrix taken at films of different oxygen content, which were annealed for 1 h at 1000 °C. In the figure, nanocrystallites are marked by circles, which represent their nearly spherical shape. As can be seen from the course of the lattice fringes imaged in these nanocrystallites, their orientation appears to be random. From HREM inspection of cross-section specimens we can state that there is no preferred nanocrystallite arrangement throughout the films. From digitized images like those shown here, the size distribution of nanocrystallites was determined for all samples of various stoichiometry. As already revealed in Fig. 1, it was found that, for equal annealing conditions, the mean nanocrystallite size is strongly correlated to the initial oxygen content of the SiO_x. The size distribution maximum clearly shifts to smaller sizes with increasing x as demonstrated by

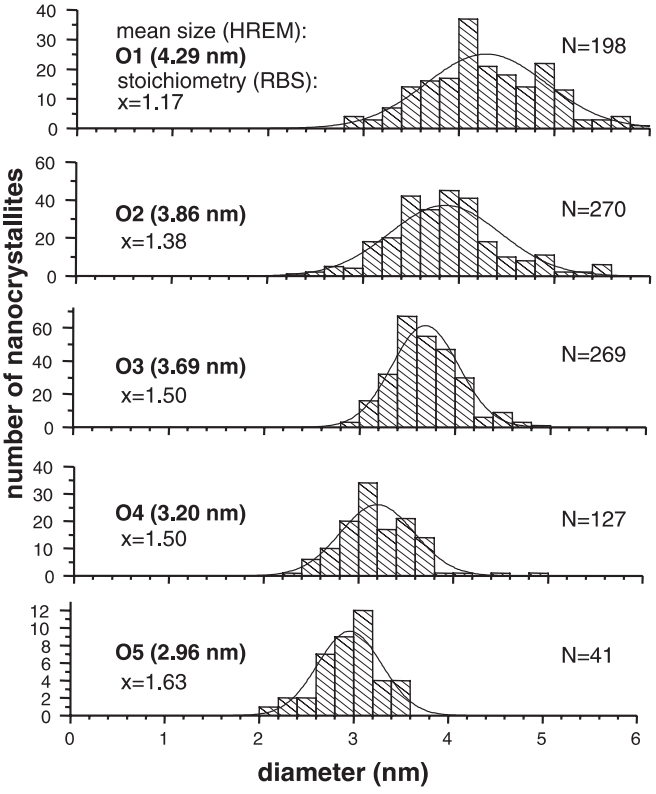

Fig. 2. Size distribution of Si nanocrystallites in SiO_x films of various oxygen content upon a 1-h annealing at 1000 °C in argon gas. The respective mean sizes as determined by electron microscopy on the basis of N nanocrystallites per sample are inserted together with the stoichiometry parameter x as determined by RBS

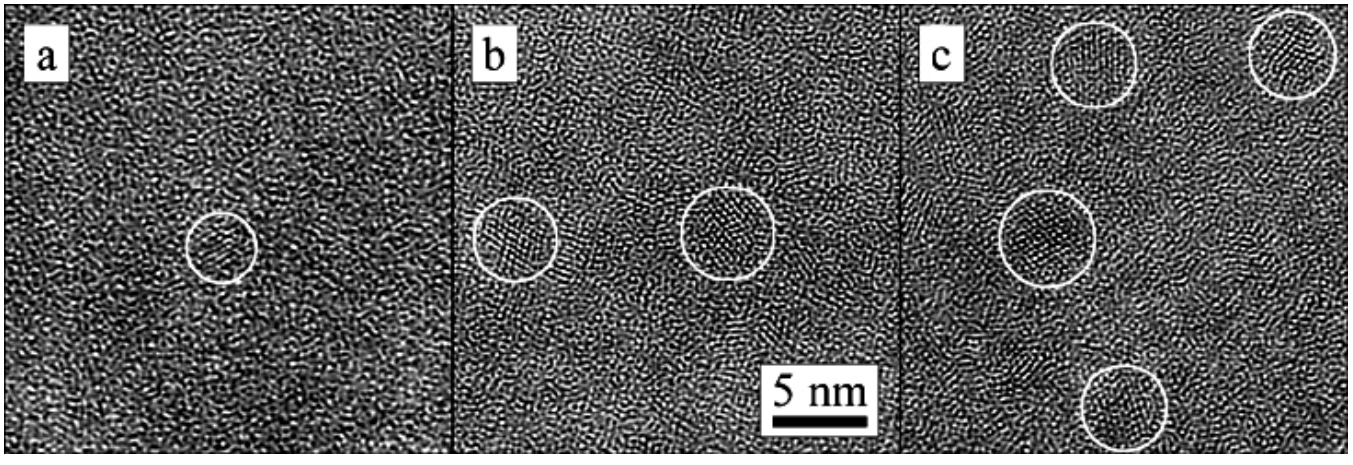

Fig. 1a–c. Representative HREM images of Si nanocrystallites formed upon 1-h annealing at 1000 °C in 100-nm–thick SiO_x films of decreasing oxygen content: **a** $x = 1.63$; **b** $x = 1.50$; and **c** $x = 1.17$. Orientation and arrangement of the nanocrystallites appear to be random

Table 1. Summary of characteristics of SiO_x films upon 1-h annealing at 1000 °C: oxygen partial pressure during evaporation, resulting O:Si ratio and x value determined by RBS, mean nanocrystallite size by HREM and PL maximum position. Because of too few nanocrystallites in O6 no mean size was derived

Sample	O_2 pressure	O:Si (RBS)	x	mean cryst. size	PL max.
O1	2×10^{-7}	54 : 46	1.17	4.3±0.64 nm	882 nm
O2	1×10^{-6}	58 : 42	1.38	3.9±0.58 nm	876 nm
O3	5×10^{-6}	60 : 40	1.50	3.7±0.35 nm	842 nm
O4	1×10^{-5}	60 : 40	1.50	3.2±0.39 nm	810 nm
O5	5×10^{-5}	62 : 38	1.63	3.0±0.34 nm	778 nm
O6	1×10^{-4}	66 : 34	2	not determined	754

Fig. 2. Accordingly, the mean nanocrystallite size achieved upon 1-h annealing at 1000 °C drops from 4.3 nm to 3 nm with the stoichiometry parameter increasing from $x = 1.2$ to $x = 1.6$. The higher oxygen content not only prevents the formation of larger nanocrystallites, but also reduces their formation rate. The highest oxygen partial pressure applied (sample O6) resulted in a stoichiometry parameter x close to 2 for which only very few crystallites could be observed. Therefore, no accurate size distribution of this sample was determined. All characteristic data of preparation, stoichiometry, structure and PL emission are summarized in Table 1.

2.2 Photoluminescence emission

SiO_x films without thermal processing (as-deposited) show only very weak PL emission with a maximum around 600 nm which redshifts upon annealing at elevated temperatures. A considerable increase in intensity up to 500 °C annealing is followed by a certain decrease up to 800 °C annealing and above. This behavior has been observed for a series of specimens of sample O1 with $x = 1.2$ as-deposited stoichiometry. The corresponding spectra are given with 20 times enlarged intensity (for better comparison with the other spectra) as dotted curves in Fig. 3. In addition to the above-mentioned loss of Si–OH and Si–H bonds upon annealing, in this temperature range IR spectroscopy also reveals structural changes due to phase separation of SiO_x into Si and SiO_2 [14]. Since no crystallization is achieved at annealing temperatures below 900 °C, the relatively weak PL emission is most probably defect-related and does not result from the presence of nanocrystallites.

The evolution of the PL signal upon annealing at even higher temperatures is demonstrated by the solid curves in Fig. 3. Upon annealing at 900 °C, the PL emission appears around 900 nm, but still at the low-intensity level of the as-deposited films. Annealing at temperatures above 900 °C gives rise to a new PL maximum positioned around 930 nm. The intensity of this peak reaches its maximum for 1050 °C annealing temperature. We attribute this characteristic emission to the presence of Si nanocrystallites, which have been proven in the films by HREM from 900 °C upwards. The evolution of PL intensity with annealing temperature in the high-temperature range, i.e. 900 °C and above, can be understood in terms of the formation of Si nanocrystallites as well as reordering of their interface to the SiO_2 matrix. While the increased annealing temperature results in an enhanced Si nanocrystallite formation rate, the interface of these nanocrystallites is expected to undergo structural rearrangements resulting in better passivation by removal of dangling bonds as proposed by López et al. [21]. The intensity drop at 1100 °C may be due either to particle growth exceeding the size limit effective for quantum confinement and/or the creation of new defects in the SiO_2 matrix.

The evolution of the characteristic red/infrared PL emission as a function of film stoichiometry has been studied on another series of specimens upon annealing at 1000 °C. The oxygen content of the as-deposited films influences the nanocrystallite size in a very specific way as shown above. Accordingly, we found changes in the spectral range of the PL emission, which may be recognized from the measurements presented in Fig. 4. In correlation with the decreasing mean size of Si nanocrystallites, we observed a continuous blueshift of the PL peak position from 882 nm for sample O1

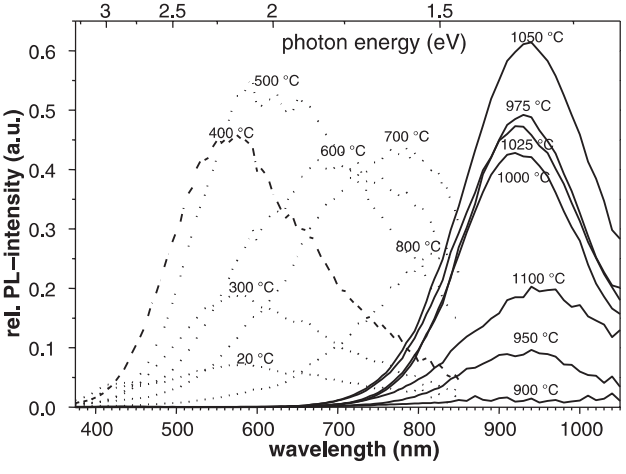

Fig. 3. UV excitation (325 nm) PL spectra of sample O1 ($x = 1.2$) measured at room temperature upon 1-h annealing at various temperatures. For better comparison the *dotted curves* are enlarged 20 times

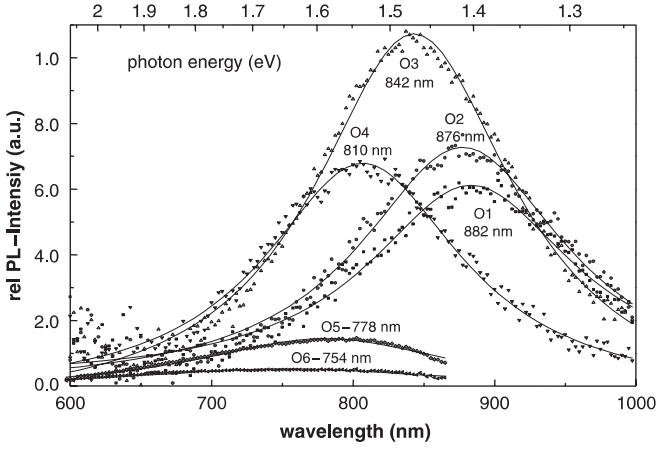

Fig. 4. UV excitation (325 nm) PL spectra upon thermal processing at 1000 °C of SiO_x films of various oxygen content. The PL emission maxima are indicated together with the sample numbers. The mean sizes of nanocrystallites in each sample correspond to those given in Table 1

with the largest to 754 nm for sample O6 with the smallest nanocrystallites. This shift would be expected from quantum confinement theory as a result of the change in particle size distribution, which influences the average bandgap in the nanocrystallites. The decrease of PL intensity accompanying the blueshift points to the reduced formation rate of nanocrystallites at higher oxygen content. In addition, we must consider that their absorption cross-section diminishes with decreasing size.

2.3 Resonant excitation photoluminescence

For the sake of clarity concerning the origin of the PL emission in high-temperature annealed SiO_x films, the resonant excitation technique at low temperature (4 K) was utilized. It is based on the assumption that, even for Si nanocrystallites, indirect recombination is the dominant mechanism. Therefore, the recombination is strongly determined by the interaction with momentum conserving phonons. For resonant excitation ($E_{ex} = E_g$) the phonon energy replicates in the PL spectra as demonstrated by Kovalev et al. [16]. The measurements were carried out on a sample having a similar composition to O4, but with a ten times larger thickness, i.e. 1000 nm, that was annealed for 1 h at 1000 °C in pure hydrogen to achieve the highest possible PL intensity. The PL spectrum of this sample resonantly excited at 845 nm is plotted as a dotted curve in Fig. 5. The positions of the expected phonon steps are marked by arrows. A rather slight shoulder about 59 meV below the excitation energy corresponds to the first transverse optical (TO) phonon step. Although it may be hardly recognized in the measured spectrum, it is clearly pronounced as a sharp peak in the first derivative of the spectrum plotted as a solid curve in Fig. 5. Even the second TO phonon step appears as a sharp peak in the derivative plot.

One reason for the weak development of phonon replica signatures in the actual spectrum is that the total PL intensity at resonant excitation is very weak and can be up to 50 000 times less than that obtained by the usual UV excitation [22]. This plays an important role, especially for nanocrystallites in an oxide matrix, since their PL intensity is generally much lower than that of porous silicon. Another reason is the limited range available for tuning the excitation energy. Whereas the PL maximum at UV excitation of this sample is around 1.5 eV, the resonant excitation energy cannot be tuned below 1.4 eV with the experimental setup used. However, in a system of nanocrystallites having a broad size distribution like ours, the excitation should be adjusted to energies significantly lower than this maximum to achieve a more distinct phonon replica signature. Nevertheless, also upon slight excitation energy variation we found repeatedly first and second phonon steps at characteristic distances relative to this energy. Accordingly, we consider the phonon energies from the Si dispersion relation replicated in the PL spectra and conclude that recombination takes place by an excitonic process within the nanocrystallites, still dominated by indirect transitions.

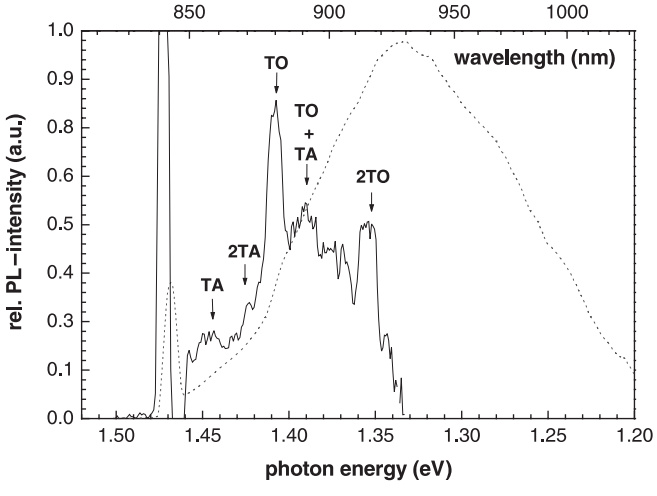

Fig. 5. Resonant excitation (845 nm) PL spectrum of sample O4 ($x = 1.5$; 3.2 nm mean Si nanocrystallite size). In addition to the actual spectrum (*dotted curve*), its first derivative (*solid curve*) is plotted with indication of the phonon steps

3 Summary

Si nanocrystallites in SiO_2 matrix were produced by reactive evaporation of SiO and subsequent annealing at elevated temperatures of the SiO_x thin films deposited onto Si-wafer substrates. The initial oxygen content of the films, and thus the mean size of the nanocrystallites formed upon high temperature processing, are controlled by the oxygen partial pressure in the vacuum chamber during film deposition. These films exhibit a characteristic PL peak around 930 nm that is strongly dependent on the presence and structural characteristics of Si nanocrystallites. The position of the PL maximum correlates with the mean size of the nanocrystallites. The origin of the PL is attributed to excitonic recombination in Si nanocrystallites due to quantum confinement. This interpretation is supported by resonant excitation PL measurements at low temperatures. Thin-film deposition by reactive evaporation of SiO and subsequent annealing at high temperatures has the advantage of a relatively easy fabrication setup and process control. This route of synthesis of Si nanocrystallites in SiO_2 matrix is thus a promising candidate for potential future applications in the production of light-emitting devices.

Acknowledgements. The authors are very grateful to Dr.D. Kovalev from the Physics Department E16 of the University of Munich, who performed the resonant excitation PL measurements. This work has been supported by the Deutsche Forschungsgemeinschaft in the framework of its priority area *Silicon Chemistry* under Grant No. Kr 1153/2-3.

References

1. L.T. Canham: Appl. Phys. Lett. **57**, 1046 (1990)
2. V. Lehmann, U. Gösele: Appl. Phys. Lett. **58**, 856 (1991)
3. T. Shimizu-Iwayama, K. Fujita, S. Nakao, K. Saitoh, T. Fujita, N. Itoh: J. Appl. Phys. **75**, 7779 (1994)
4. J. Linnros, A. Galeckas, N. Lalic, V. Grivickas: Thin Solid Films **297**, 167 (1997)
5. S. Hayashi, Y. Kanzawa, T. Kageyama, S. Takeoka, M. Fujii, K. Yamamoto: Solid State Commun. **102**, 533 (1997)
6. R.K. Soni, L.F. Fonseca, O. Resta, M. Buzaianu, S.Z. Weisz: J. Luminesc. **83–84**, 6128 (1999)
7. K. Murakami, T. Suzuki, T. Makimura, M. Tamura: Appl. Phys. A **69** (Suppl.), S13 (1999)
8. L. Patrone, D. Nelson, V.I. Safarov, S. Giorgio, M. Sentis, W. Marine: Appl. Phys. A **69** (Suppl.), S217 (1999)

9. H. Hofmeister, P. Ködderitzsch, J. Dutta: J. Non-Crystalline Solids **232**–**234**, 182 (1998)
10. H. Hofmeister, P. Ködderitzsch: Nanostructured Materials **12**, 203 (1999)
11. T. Inokuma, Y. Wakayama, T. Muramato, R. Aoki, Y. Kurata, S. Hasegawa: J. Appl. Phys. **83**, 2228 (1998)
12. F. Iacona, G. Franzò, C. Spinella: J. Appl. Phys. **87**, 1295 (2000)
13. U. Kahler, H. Hofmeister: Appl. Phys. Lett. **75**, 1765 (1999)
14. U. Kahler, H. Hofmeister: Materials Science Forum **343**–**346**, 488 (2000)
15. U. Kahler, H. Hofmeister: Optical Materials **17**, 83 (2001)
16. D. Kovalev, H. Heckler, M. Ben-Chorin, G. Polisski, M. Schwartzkopff, F. Koch: Phys. Rev. Lett. **81**, 2803 (1998)
17. P.D.J. Calcott, K.J. Nash, L.T. Canham, M.J. Kane, D. Brumhead: J. Physics: Condens. Matter **5**, L91 (1993)
18. D. Vick, L.J. Friedrich, S.K. Dew, M.J. Brett, K. Robbie, M. Seto, T. Smy: Thin Solid Films **339**, 88 (1999)
19. U. Kahler: Ph.D. Thesis (Martin-Luther University, Halle 2001)
20. W.A. Pliskin, H.S. Lehmann: J. Electrochem. Soc. **112**, 1013 (1965)
21. M. López, B. Garrido, C. Bonafos, A. Pérez-Rodríguez, J.R. Morante, A. Claverie: Nucl. Instrum. Methods Phys. Research B **178**, 89 (2001)
22. D. Kovalev, H. Heckler, G. Polisski, F. Koch: Phys. Status Solidi B **215**, 871 (1999)